

IMPACT OF PVA FIBER AS FINE AGGREGATE REPLACEMENT IN ALKALI-ACTIVATED FLY ASH ON FLOW RATE, MECHANICAL PROPERTIES AND DRYING SHRINKAGE

* Yuyun Tajunnisa¹, Wahyuniarsih Sutrisno² and Mitsuhiro Shigeishi³

¹Department of Civil Infrastructure Engineering, Institut Teknologi Sepuluh Nopember, Surabaya, Indonesia

²Department of Civil Engineering, Institut Teknologi Sepuluh Nopember, Surabaya, Indonesia

³Department of Civil and Environmental Engineering, Kumamoto University, Kumamoto, Japan

*Corresponding Author, Received: 24 Feb. 2019, Revised: 27 March 2019, Accepted: 30 April 2019

ABSTRACT: This study focuses to discuss the performance of alkali-activated mortar (AAM) reinforced by Polyvinyl Alcohol (PVA) fiber as a replacement of fine aggregate. Drying shrinkage is a major problem of alkali-activated mortar (AAM). Therefore, in order to reduce shrinkage and improve the performance of the mortar; the Polyvinyl Alcohol (PVA) fiber was introduced to replace the fine aggregate. An experimental test, including flow rate, compressive strength, modulus elasticity, poisson's ratio, flexural strength and rate of drying shrinkage, was performed to investigate the performance of AAM with various percentage of PVA fiber. Based on the test, it was obtained that the utilization of PVA fiber as a fine aggregate replacement shows a slight decrease in the flow rate compared to plain AAM. The density of PVA AAM reinforced-fiber of five mixtures is almost similar to plain AAM with the differences lower than 2%. The use of PVA at levels ranging from 0% to 2%, with a level increment of 0.5% by volume, as fine aggregate replacement increased compressive strength, but decreased flexural strength. The replacement of fine aggregate with a certain value of PVA, which are 0.5% by volume, reduces the drying shrinkage of mortar. However, adding PVA more 0.5% by volume to the mortar increases the drying shrinkage.

Keywords: Alkali-activated materials, Slag, Fly ash, Fiber, Drying shrinkage.

1. INTRODUCTION

The application of alkali-activated materials, which also often called AAMs, in the concrete industry, has been increasing significantly in recent years. These materials, which known since 1908, present better compressive strength, low permeability, high-temperature resistance, frost resistance, higher early strength, and higher acid resistance compared with Portland cement [1-4]. Additionally, AAMs production does not entail high temperature and is able to be formed at ambient temperature [5]. Furthermore, the shrinkage of AAMs is less compared to Portland cement and it also attains higher unconfined compressive strength [6-7].

The fiber-reinforced composite (FRC) made from short polyvinyl alcohol (PVA) has been proved to have good flexural strength and equitable properties [8-9]. Ohno and Li [10] investigated the FRC with the incorporation of PVA fiber to fly ash based geopolymer could improve both strength and ductility properties with strain hardening tensile ductility over 4%.

The shrinkage properties of geopolymer concrete are one of the most characteristics that affect the performance of the concrete [11-12]. Juarez [13] reported plastic shrinkage cracking in a cementitious matrix during the drying stage using

both PVA and natural fiber. These fibers as reinforcement in cement-based mortars reduce plastic shrinkage. Moreover, increasing of fiber number per unit volume demonstrates reducing the total cracking area at least 93% of the total cracking area compared with mortars without fibers. In addition, PVA fiber is more effective at matrices prepared with low water/binder ratios [14].

Hamoush [15] in his research found that the PVA fiber can be used as a fiber-reinforced composite (FRC) in concrete. The bond between matrix and fiber of concrete using PVA is very strong. This condition happened because of high chemical bonding between these two materials resulting rupture of micro-fiber. Zhao et al [16] recently reported that the addition of 10% volume of short fibers into the concrete increases the flexural strength of geopolymer matrix by 224%. [17]

Previous researchers found PVA fibers were employed with a volume fraction of f %, by adding f % fiber in the mixture, which f % is a percentage value of total mixture volume. Thus, fibers addition changes the total volume of the mixture, and reducing the workability of the mixture. Therefore, this study proposes the utilization of PVA fiber as a replacement of fine aggregate, not as the addition of mixture. Mixture volume after fiber addition is fixed, not changed. It is expected that mixture

workability will not reduce. This study investigates the effect of PVA short fiber as ‘fine aggregate replacement’ on fly ash-activated mortar replaced by 42.5% ground granulated blast furnace slag (GGBFS) and 15% micro silica (M) on mechanical properties and drying shrinkage. Mix design of alkali-activated mortar (AAM) was developed based on a previous study [23] found that AAM-VI with 42.5% fly ash/42.5% GGBFS/ 15% M - has a highest compressive strength, higher flexural strength and better microstructure among other AAM mixtures; conversely, AAM-VI has higher drying shrinkage compared with OPC mortar.

2. MATERIALS AND EXPERIMENTAL SETUP

In this paper, the experimental test was performed to investigate the mechanical properties and shrinkage behavior of AAMs mortar compared with the OPC mortar. The detail of material and experimental set up explained at the next sub chapter below.

2.1 Materials and Mixture Proportion

The materials used in this experimental test was AAMs mortar which consists of Class F Fly Ash (FA), Ground Granulated Blast Furnace Slag (GGBFS) with a specific surface area of 4000-4120 cm^2/g ; and un-densified micro-silica (M) with Grade 940 as [18]. Furthermore, the alkaline solution for this mixture was a poly-carboxylic acid ether-based agent, which has high-performance air entrained and water reducing agent. Standardized sand, as reported in [19-20], was used as the fine aggregate. For the first test, the flow rate test was performed to select the most representative mixture based on their flow behavior.

The AAM mixture was added with various percentages of PVA fiber range from 0.5% until 2% of total AAM volume. The specific gravity and chemical composition of materials are listed in Table 1. The ratio of FA: GGBFS: M used in this mixture is 42.5:42.5:15. Solid precursors were mixed with alkali solution which is sodium silicate and 8 molar sodium hydroxide with a ratio of 1.5. The liquid consists of the alkaline solution and air entrained agent. Total 2% of solid precursor mass was used as the mass of air entrained-agent. The ratios of liquid and alkaline solution per solid precursor were fixed at 0.558 and 0.538 by weight for all AAM mixtures respectively [24].

The solid precursors of AAM-IV mixture proportions are given in Table 2. All specimens of fiber-reinforced mortar were examined for their performance including flow-rate, compressive and flexural strength and also drying shrinkage behavior. The freshly mixed mortar was used for flow rate test. Compressive strength test used a cylinder of 50 x

100 mm. There are also prismatic specimens of 40 x 40 x 160 mm, which used for flexural test and drying shrinkage test.

2.2 Experimental Procedure

The mixture procedure of reinforced fiber composite mortar was performed in the two liter-batch mixer in the control room at temperature 18-20° C and RH of 70-99.9%. The solid precursors were mixed for two minutes at low speed. Further, the 8 M sodium hydroxide solution was dissolved at least one day before mortar mixing and then mixed manually with sodium silicate gel for five minutes. After this procedure, the mixture was rested for ten minutes and the mixing process was continued with the addition of air entrained-agent. The alkaline liquid mixed with the solid precursors for about two minutes at low speed. After two minutes of mixing, the mixer was stopped and the standardized sands were added. The mixing process was continued for 3 minutes low-speed mixing configuration and then PVA fiber was carefully added to the mixture and continued for another three minutes low-speed mixing. After the mixing process finished, the flow ability test was performed for each mixture. The flow rate was tested twice for each mixture as [19] corresponding to [21].



Fig 1. Flexural test on mortar reinforced fiber composite (A) before and (B) after failure



Fig 2. Compressive test and drying shrinkage test on mortar reinforced fiber composite specimens

Each mortar was cast immediately into three 40x40x160 mm prismatic molds and 50x100 mm cylindrical molds after performing the flow rate test. All molds were compacted on the vibrator for approximately 2 minutes to remove air bubbles. For the next step, all prismatic and cylindrical specimens were cured in the air at a temperature of

18-20°C and relative humidity of 70-99.9% with the unsealed condition. After two days, all specimens were demolded and continued to unseal cured in the air prior to the testing date.

Flexural and compressive test, as shown in Fig 1, was conducted for prisms at 28 days as [19].

Cylindrical compression tests were performed at 28 days as [22]. After demolding, the drying shrinkage test, as shown in Fig. 2, was conducted for three prisms with 40x40x160 mm dimension up to 30 days.

Table 1. The chemical analysis and specific gravity (SG) [24]

Materials	Chemical Compound (% weight)							SG (g/cc)
	SiO ₂	Al ₂ O ₃	Fe ₂ O ₃	CaO	Na ₂ O	H ₂ O	K ₂ O	
JFA-ash	55.19	25.35	7.57	4.06	-	-	-	2.33
GGBFS	35	16	0.7	46	-	-	-	2.89
Micro silica	93.67	0.83	1.3	0.31	0.4	-	-	2.22
Standardized Sand*	98.4	0.41	0.36	0.16	0.01	<0.2	0.01	2.64
OP cement								3.16
Na ₂ SiO ₃ gel								1.6
NaOH solution								1.22
Air entrained-agent								1

Table 1. Solid precursors of AAM Compositions [24]

Mortar	Symbols	JFA-FA (%)	GGBFS (%)	M (%)
AAM-I	FA ₅₀ S ₅₀	50	50	0
AAM-II	FA ₉₀ M ₁₀	90	0	10
AAM-III	FA ₄₀ S ₅₀ M ₁₀	40	50	10
AAM-IV	FA _{47.5} S _{47.5} M ₅	47.5	47.5	5
AAM-V	FA ₄₅ S ₄₅ M ₁₀	45	45	10
AAM-VI	FA _{42.5} S _{42.5} M ₁₅	42.5	42.5	15
AAM-VII	FA ₄₀ S ₄₀ M ₂₀	40	40	20
OPC	As reference			

Note: this table shows the proportion of solid precursors by weight of alkali-activated mortars with supplementary materials such as S= GGBFS, FA = fly ash, OPC=Ordinary Portland Cement and M= micro-silica

3. RESULT AND DISCUSSION

3.1 Flow Rate and Density of Specimens

The flow rate of each fiber-reinforced mortar mixture AAM-F was measured every fifteen strokes. The average values of the measured diameter of specimens on the flow test were presented in Figure 3. Test result expresses that diameter of mortar specimens is slightly increased as stroke number increase. The lowest final flow rate is shown by specimens AAM-F2.5 which only increased 5 mm in sixty strokes. This specimen also has the lowest initial flow rate compared with the other AAM-F specimens. However, the best initial and final flow rate was presented by specimens AAM-F0.5 which shows diameter for an initial flow rate of 282 mm and it increased 66 mm by the number of strokes. This result is expected due to the smaller volume of fiber which added into the mixture.

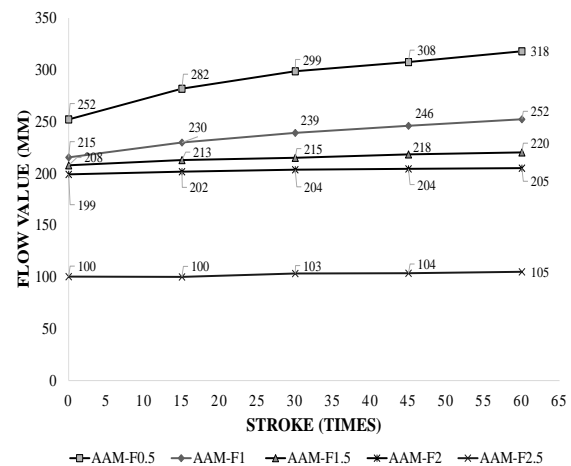


Fig. 3 Graph of flow rate vs. stroke of mortar reinforced fiber composite on flow ability test

Three of the most representative mixture were selected for strength and drying shrinkage test based on the flow rate test result to avoid the stiff and

unflowable mixture. The AAM-F2.5 have very low flow rate value, so it was difficult to mix, transport, place and compact. Therefore, the mixing properties of AAM-F0.5, AAM-F1, and AAM-F2 were then selected for strength and drying shrinkage test due to their reasonable flow rate value.

The average densities of each reinforced fiber composite mortar were presented in Table 3. The density was calculated by measuring the weight of each prism at the 28-day. The average density of each specimen is 2.23 g/cm³, 2.91 and 2.95 g/cm³ for AAM-F0.5, AAM-F1 and AAM-F2, respectively. The error rates of each result are below 2% compared with the averaged measured values. Meanwhile, cylindrical specimens have similar trend result of average density compared to prism specimens.

Table 3 Density of AAM-F prisms

Prismatic Specimen Code	Weight (g)	Density (g/cm ³)	Average (g/cm ³)
AAMF-0.5-1	593.4	2.24	2.23
AAMF-0.5-2	601.8	2.23	
AAMF-0.5-3	602.2	2.22	
AAMF-1-1	597.0	2.84	2.91
AAMF-1-2	589.0	2.94	
AAMF-1-3	604.0	2.94	
AAMF-2-1	602.1	2.91	2.95
AAMF-2-2	598.8	2.92	
AAMF-2-3	599.4	3.01	

3.2 Stress-Strain Relationship of Cylinder Specimens

The compressive stress-strain relationship of cylindrical specimens of AMM-F mortar was investigated by using compressive tests with strain gauges attached vertically and horizontally at the surface of the specimen. Stress-strain transversal and longitudinal of each mixture were measured and plotted as shown in Figure 4 and Figure 5.

The transversal stress-strain of composites PVA mortar was plotted in Figure 4. It was shown that the axial compressive curves are almost linear for three specimens. The maximum of strain as recorded by strain gauge was range from 0.0028 to 0.0034 which is similar to normal OPC concrete 0.003 as reported by [20]. After the peak stress was reached, a sudden failure occurred. The specimen with 1% addition of PVA fiber (AAM-F1) has the highest strain, followed by the sample with 2% (AAM-F2) and 0.5 % PVA fiber (AAM-F0.5).

Further, it also observed that PVA fibers enhanced the cracking response of the geopolymer mortar specimen. The stress-strain response as shown in Figure 4 proves that specimens with PVA

fibers exhibited the ability to accommodate higher strain level.

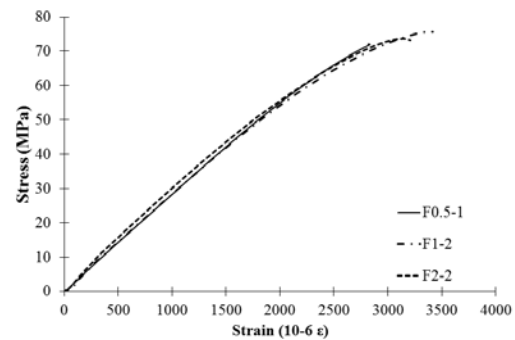


Fig. 4 Stress-strain transversal observed from vertically placed strain gauges

Subsequently, the longitudinal stress-strain of composites PVA mortar subjected to axial compression, as shown in Figure 5, shows the curves is linear in elastic condition then followed by plastic condition until reach maximum strength similar with moment curvature of concrete which is linear with the study of [21]. The maximum strain showed with the value of strain record observed by strain gauges ranged from 0.0016 to 0.0036. The highest strain provided with the addition of 2% PVA fiber. The longitudinal stress-strain response in Fig. 5 shows that specimens with PVA fibers provided the ability to accommodate higher strain level until their peak stress level.

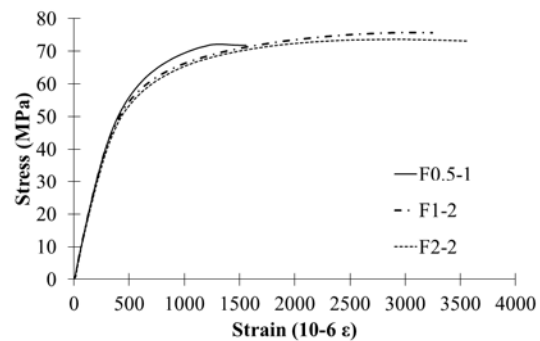


Fig. 5 Stress-strain longitudinal observed from vertically placed strain gauges

3.3 Modulus of Elasticity and Poisson's Ratio

The observed value of modulus elasticity and Poisson's ratio for mixtures F0.5, F1 and F2 are shown in Table 5 and Fig. 6. The addition of fiber to the mixture, as expected can increase the modulus of elasticity of the sample. This condition also followed with the increase of compressive strength of the sample. However, the experimental results also indicate that the increase of the modulus

of elasticity due to the addition of the mortar was not significant. It was represented by a slight increase, which is around 3%, for each replacement. These outcomes were also previously reported by researchers [23] using different types of fibers with various modulus of elasticity. From the result, it was found that the modulus of elasticity of the fiber does not significantly affect the values of concrete static elastic modulus. Furthermore, adding more fibers and applied the longer type of fiber can reduce the concrete modulus of elasticity.

Table 5. The Poisson's ratio and Modulus of elasticity of AAM-F

Type	Compressive Strength (MPa)	Stroke Max (mm)	Modulus of Elasticity (E, Gpa)	Poisson Ratio (v)
F0.5-1	72.12	0.74	28.61	0.19
F1-2	75.66	0.80	29.05	0.19
F2-2	73.69	0.82	30.54	0.21

The Poisson's ratio of fiber geopolymer mortar (AAM-F) obtained from the experimental result was lay between 0.19 and 0.21 as shown in Table 5. This value is similar to concrete made from Portland cement which has Poisson's ratio ranged from 0.11 to 0.22.

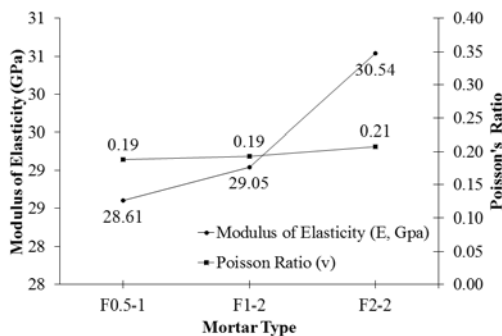


Fig. 6 Modulus of Elasticity and Poisson's Ratio of AAM-F

3.4 The Compressive Strength of Prism Sample

The compressive test was performed for cylinder and prism specimens. The compressive test for prism specimens used the unbroken part of prism samples after the flexural test. As expected from the content of fiber ratio used, mixture AAM-F2-2 showed the highest compressive strength followed by mixture AAM-F1-2. The result implies that as the fiber percentage increased, the compressive strength increased. Fig. 7 illustrates the average compressive strength of all specimens. The AAM-VI is plain geopolymer mortar as a reference to control fiber mortar AAM-F [24]. Fig. 8 illustrates average compressive strength for cylinder specimens which have the same composition with prismatic samples. Even though,

prismatic results of AAM-F1 and AAM-F2 have higher compressive strength of about 12% than those of cylindrical sample results. It shows the similar tendency of those of prisms that as the fiber percentage increase the compressive strength increased. Therefore, it can be concluded that the addition of PVA fiber with a certain amount can increase the compressive strength of AAM mortar.

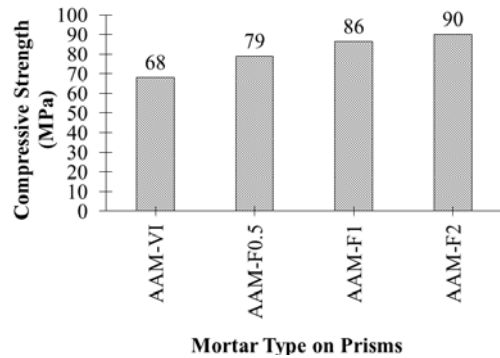


Fig. 7 The average 28-day-compressive strength of geopolymer mortar fiber reinforced composite (AAM-F) of prism specimens

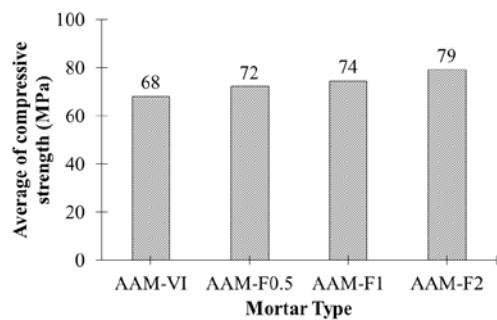


Fig. 8 The 28-day compressive strength of geopolymer mortar fiber reinforced composite (AAM-F) of cylindrical specimens

All fiber specimens (AAM-F) showed different fracture behaviors compared with that of plain mortar (AAM-VI). It was observed that the propagation of cracks was restrained due to fiber action. Furthermore, the original shape of AMM-F specimens is remained intact after loading reach the highest value as shown in Fig. 9.



Fig. 9 An example shape of prismatic specimens remained after compressive loading at (A) plain geopolymer mortar (AAM-VI) and (B) geopolymer fiber reinforced composite (AAM-F).

3.5 Flexural Strength

The 28 day-flexural strength of three geopolymer composite mixes are listed in Table 6. The sample AAM-F0.5 shows the highest cracking moment, followed by AAM-F1, AAM-F2, and AAM-VI. According to compressive results of prisms, it reveals that as the fiber content increase the compressive strength also increased, but the flexural strength decreased. This result does not follow the prediction which the higher amount of fiber may reach higher flexural moment capacity due to fiber strength. In this study, the addition of fiber is performed by replacing sand in the mortar.

Actually, there are two rules for adding fiber. The first rule is fiber was just added to the mixture which causes the volume fraction of fiber content increased. This condition cause at a certain range addition of fiber, compressive strength can increase until maximum workable mortar reached. Then, strength decreased after workability reduced. For the second rule, the total volume of mortar must be constant. This condition caused the mortar density decreased slightly since the density of fine aggregate is higher than the fiber. Furthermore, the workability also increased until the addition of certain volume of fiber. According to the result, the compressive and flexural strength of AAM mortar are related to density, workability, and combination of fiber and sand at a certain range.

Therefore, the reason for the higher flexural strength of AAM-F0.5 compared to AAM-F1 and AAM-F2 are associated with the highest flowability of AAM-F0.5 among other AAM-F mixtures. Thus, it causes easy compaction, leading to higher flexural strength, compared with AAM-F1 and AAM-F2.

3.6 Drying Shrinkage

The result of drying shrinkage test was shown in Figure 10. After 30 days test, the smallest drying shrinkage reached at 560 mm is AAM-F0.5; followed by AAM-F1 at 840 mm; then the highest is AAM-F2 at 1090 mm. This shrinkage value is comparatively low compare with the same AAM specimens without PVA fiber which has drying shrinkage value of 1200 mm. Furthermore, the OPC mortar has a drying shrinkage value of 840 mm at 30 days which is the same with AAM-F1. Therefore, it can be concluded that PVA fiber can reduce drying shrinkage value. It also obtained from the result that the optimum amount of PVA fiber replacement is 0.5%. Adding more PVA fiber to the mixture as a fine aggregate replacement can increase the drying shrinkage value. This condition is because the characteristic of PVA which has a tendency to absorb more water during the fresh stage of mortar, so the chance of an increase in drying shrinkage is bigger when more fiber is added into the mixture.

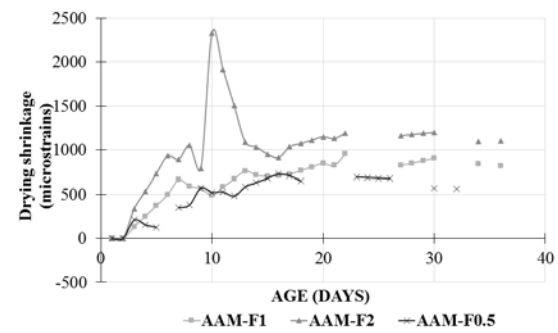


Fig. 10 Drying Shrinkage of AAM-F Specimens

Table 6. Flexural test result

Prismatic Sample	Length (mm)	height (mm)	width (mm)	W (mm ²)	Load (kN)	Moment (Nmm)	Flexural strength (MPa)	Average Flexural Strength (MPa)
AAM-F0.5-1	160.3	39.9	41.5	11009.1	5.8	144500.0	13.13	
AAM-F0.5-2	160.3	39.9	42.3	11219.8	5.5	137750.0	12.28	12.7
AAM-F0.5-3	160.3	39.9	42.5	11276.9	5.8	144000.0	12.77	
AAM-F1-1	121.0	40.2	43.2	11634.5	5.6	139250.0	11.97	
AAM-F1-2	121.0	39.9	41.5	11019.9	4.6	113750.0	10.32	10.9
AAM-F1-3	120.8	40.2	42.3	11369.8	4.7	117000.0	10.29	
AAM-F2-1	121.2	40.1	42.6	11423.2	4.8	120000.0	10.50	
AAM-F2-2	121.2	40.2	42.1	11342.4	4.4	109250.0	9.63	10.1
AAM-F2-3	120.7	38.5	42.8	10591.9	4.3	106500.0	10.05	
AMM-VI	Reference Specimen [24]							8.9

4. CONCLUSIONS

Series of the experimental test was performed to investigate mechanical performance and drying shrinkage behavior of alkali-activated mortar reinforced by PVA fiber. Based on the experimental test it was found that the utilization of PVA fiber gives a slight decrease to the flow ability of mortar compared with typical mortar. Furthermore, the density of PVA mortar fiber of all mixture was equal to typically geopolymer mortar with difference below 2%. The addition of PVA mortar to the mixture slightly increase the compressive strength and strain of the mortar specimens. However, the results of the flexural and drying shrinkage test showed a slightly different manner. Addition of fiber above 0.5% has been proven to reduce flexural strength and the drying shrinkage of mortar specimens, but adding PVA more 0.5% by volume to the mortar can increase the drying shrinkage.

5. REFERENCES

- [1] Provis J. and Deventer J.V., Structures, Processing, Properties, and Industrial Applications, Woodhead Publishing Limited, 2009, ISBN: 978-1-84569-449-4, pp. 2-21.
- [2] Law, D.W., Adam, A.A., Molyneaux, T.K. et al., Long Term Durability Properties of Class F Fly Ash Geopolymer Concrete, Mater. Struct., Vol. 48, Issue 3, 2015, pp. 721–731.
- [3] Nyuyen H.Q. Lorente S., Bareone A.D., Lamotte H., “Porous Arrangement and Transport Properties of Geopolymers”, Construction, and Building Materials, Vol. 191, 2018, pp. 853 –865.
- [4] Xu F., Deng X., Peng C., Zhu J., Chen J., Mix Design and Flexural Toughness of PVA Fiber Reinforced Fly Ash-Geopolymer Composites, Construction and Building Materials, Vol. 150, 2017, pp. 179–189.
- [5] Temuujin J., Williams R. and Riessen V. A., “Effect of Mechanical Activation of Fly Ash on The Properties of Geopolymer Cured At Ambient Temperature, Journal of Materials Processing Technology, Vol. 209, Issue 12-13, 2009, pp. 5276–5280.
- [6] Savastano H J., Warden P., and Coutts R., Potential of Alternative Fibre Cement As Building Materials For Developing Areas, Cement and Concrete Resources, Vol. 25, Issue 6, 2003, pp. 585–592.
- [7] Dias P. D. and Thaumaturgo C., The Fracture Toughness of Geopolymeric Concrete Reinforced With Basalt Fibers, Cement and Concrete Composite, Vol. 27, 2003, pp. 49–54.
- [8] Yunsheng Z., Wei S. and Zongjin L., Impact Behavior and Microstructural Characteristics of PVA Fiber Reinforced Fly Ash-Geopolymer Boards Prepared by Extrusion Technique, Journal of Material Science, Vol. 41, Issue 10, 2006, pp. 2787-2794.
- [9] Xu S., Malik M.A., et. al., Influence of the PVA Fibers And SiO₂ Nps on The Structural Properties Of Fly Ash Based Sustainable Geopolymer. Construction and Building Materials, Vol. 164, 2018, pp. 238–245.
- [10] Ohno M. and Li V. C., A Feasibility Study of Strain Hardening Fiber Reinforced Fly Ash-Based Geopolymer Composites, Construction and Building Materials, Vol. 57, 2014, pp. 163–168.
- [11] Castel A., Foster S.J., Ng T. et al. Creep And Drying Shrinkage of A Blended Slag And Low Calcium Fly Ash Geopolymer Concrete, Materials Structures, Vol. 49, Issue 5, 2016, pp. 1619-1628.
- [12] Singh B., Ishwarya G., Gupta M., Bhattacharyya S. K., Geopolymer Concrete: A Review of Some Recent Developments. Construction and Building Materials, Vol. 85, 2015, pp. 78–90.
- [13] Juarez C. A., Fajardo G., Monroya S., Duran-Herrera A., Valdez P. and Magniont C., Comparative Study Between Natural And PVA Fibers to Reduce Plastic Shrinkage Cracking in Cement-Based Composite, Construction, and Building Materials journal, Vol. 91 , 2015, pp. 164–170.
- [14] Felekoglu B., Tosun-Felekoglu K., Keskinates M., and Gödek E., A Comparative Study on The Compatibility of PVA And HTPP Fibers With Various Cementitious Matrices Under Flexural Loads, Construction and Building Materials, Vol. 121, 2016, pp. 423-428.
- [15] Hamoush S., Abu-Lebdeh T., and Cummins T., Deflection Behavior of Concrete Beams Reinforced With PVA Micro-Fiber, Construction and Building Materials, Vol. 24, Issue 11, 2010, pp. 2285–2293.
- [16] Zhao Q., Nair B., Rahimian T. and Balaguru P., Novel Geopolymer Based Composites with Enhanced Ductility, Journal of Material Science, Vol. 42, Issue 9, 2007, pp. 3131-3137.
- [17] Giancaspro J., Ph.D. Thesis, Rutgers University, 2004, pp. 513.
- [18] JIS A 6207 Silica fume for use in concrete, 2016.
- [19] JIS R 5201 Physical testing methods for cement, 2015.
- [20] Chemical analysis CAJS I-12, Association Japan Cement, 1981.
- [21] JIS A 1108 Standard for compression of the cylinder, 2006.
- [22] ISO 1920-4, 2005.
- [23] Tajunnisa, Y., et. al., Performance Of Alkali-Activated Fly Ash Incorporated With GGBFS And Micro-Silica In The Interfacial Transition Zone, Microstructure, Flowability, Mechanical Properties And Drying Shrinkage, AIP Conference Proceedings, 2017, pp188-199.
- [24] Tajunnisa, Y., et. al., Effect of GGBFS and Micro-Silica on Mechanical Properties, Shrinkage and Microstructure of Alkali Activated Fly Ash Mortar., International Journal of GEOMATE, Vol.13, Issue 36, 2017, pp.100-107.